STRUCTURAL MODELING AND FUNCTIONAL PREDICTION OF IFN-Y GENE VARIANTS

 $\begin{array}{l} \text{Bilal, I.}^1 - \text{Munir, H.}^{2^*} - \text{Ramzan, K.}^1 - \text{Zulfiqar, I.}^3 - \text{Waheed, A.}^1 - \text{Haider, A.}^4 - \text{Ali, F.}^5 \end{array}$

¹ Department of Biochemistry, University of Okara, Okara, Pakistan.

² Department of Molecular Biology, University of Okara, Okara, Pakistan.

³ Center for Applied Molecular Biology (CAMB), University of Punjab, Lahore, Pakistan.

⁴ Department of Biotechnology, University of Okara, Okara, Pakistan.

⁵ Department of Chemistry, GC University Faisalabad, Faisalabad, Pakistan.

*Corresponding author e-mail: haris.munir.visiting[at]uo.edu.pk

(Received 28th February 2025; revised 03rd June 2025; accepted 11th June 2025)

Abstract. IFN-γ is a key immunomodulatory cytokine primarily secreted by activated T lymphocytes, NK cells, NKT cells, and dendritic cells. The IFN-γ protein is encoded by the IFNG gene located on chromosome 9q14.3 and plays a central role in host immune responses. The current study employed an integrated computational approach to predict deleterious missense SNPs of the IFN-y gene. These variants potentially disrupt the structural integrity and biological activity of IFN-y, contributing to aberrant immune responses implicated in tumorigenesis and chronic inflammation. To assess the functional consequences of these mutations, molecular docking analyses were conducted. Through comprehensive screening, 12 deleterious nsSNPs were identified, localized within non-synonymous regions. SOPMA revealed that the IFN-γ protein is predominantly α-helical, constituting about 66.27% of the total secondary structure. Our results show high disorder scores for the G161R, R152Q, M1L, and A164S mutants, suggesting a loss of structural order, which may negatively impact protein function. Structural modeling was performed using AlphaFold, followed by validation with the SAVES v6.0 server, K28T, Y37C, and Y76F induced marked conformational changes involved in receptor binding, as evidenced by high RMSD values. Our results emphasize Laminin, Tamoxifen, Fulvestrant, Melanin, Parecoxib, and Rofecoxib, Both Laminin and Melanin demonstrated strong binding affinities with native and mutant IFN-y structures, engaging crucial residues such as Phe115, Glu116, Phe105, and Val73. These residues are crucial for ligand binding and cytokine function, highlighting their therapeutic importance. Our findings provide insights for the development of targeted therapies for IFN-γ-related disorders, including autoimmune diseases, cancer, and infectious conditions. The novelty of this study lies in its comprehensive analysis of mutant IFN-γ forms, paving the way for precision medicine approaches tailored to genetically diverse populations. Further experimental validation is necessary to substantiate these findings and evaluate their clinical significance.

Keywords: cytokine, IFNG, NKT cells, non-synonymous SNPs

Introduction

Single-nucleotide polymorphisms (SNPs) in the interferon-gamma (IFN- γ) gene are key tumor progression and suppression regulators. This gene is primarily expressed in immune cells such as antigen-activated T cells, natural killer (NK) cells, natural killer T (NKT) cells, and dendritic cells (DCs). Moreover, the production of IFN- γ can be indirectly triggered by lipopolysaccharides (LPS) and certain viral infections. In 1957, the term "Interferon" (IFN) was first coined to describe a substance that inhibited the

spread of the influenza virus in an experimental study conducted on mice (Isaacs and Lindenmann, 1957). This discovery led to the identification of a new family of proteins known as IFNs, which are classified into three types; Type I (IFN- α), Type II (IFN- γ), and Type III, also referred to as IFN-λ including IFN-λ1, IFN-λ2, and IFN-λ3, formerly known as IL-28A and IL-28B (Khanna and Gerriets, 2020). Type I IFN genes are present in all vertebrates and are generally large and intronless. IFN-α1 and IFN-α13 share a high degree of sequence similarity, while IFN- β , IFN- ω , IFN- κ , and IFN- ϵ exist as single genes with minimal amino acid homology among them. The 13 IFN-α genes encode 12 structurally identical IFN-α proteins. In amphibians, IFN genes may either be intronless or contain introns (Kotenko and Durbin, 2017; Sang et al., 2016; Qi et al., 2010). The IFN-γ gene is situated on chromosome 12q14.1 and comprises 4 exons and 3 introns, covering approximately 9.6 Kb between base pairs 57,700,000 and 67,300,000. It encodes interferon-gamma (IFN-γ), a vital cytokine involved in immune defense. IFN-γ is initially synthesized as a monomer with 146 amino acids but undergoes posttranslational modifications to form a functional homodimer consisting of 166 amino acids (Reynard, 2002). Structurally, it belongs to the type II IFN family and features a helical arrangement with 6 α-helices necessary for receptor interaction. The regulation of IFN-γ expression is influenced by promoter regions and untranslated regions (UTRs), which provide binding sites for transcription factors (STAT1, NF-κB, and IRF-1). These elements play a key role in controlling IFN-y production in response to immune challenges, including infections and inflammatory conditions (Savan et al., 2009). One distinctive characteristic of IFN-y is its conserved C-terminal tail, which is present across various species such as fish, frogs, chickens, and mammals. This region contains lysine and arginine residues, which contribute to its biological function (Griggs et al., 1992).

Genome-wide association studies (GWAS) have identified several SNPs in the IFN-y gene that can lead to altered immune responses, increasing susceptibility to various infectious diseases, autoimmune disorders, and inflammatory conditions (Kaur et al., 2019). According to data from the Catalogue of Somatic Mutations in Cancer (COSMIC), among 49,967 unique samples analyzed, 243 unique samples exhibited IFN-γ mutations. These mutations can impact IFN-γ production, receptor binding, and downstream signaling pathways, ultimately disrupting immune regulation. Notably, the rs1861494 SNP has been linked to leprosy, asthma, and non-Hodgkin lymphoma. Moreover, the rs2069718 SNP has been associated with critical cases of COVID-19, suggesting a potential role in disease severity. The rs2430561 SNP has been implicated in susceptibility to tuberculosis, highlighting its significance in immune response regulation (Pacheco and Moraes, 2009). These mutations can impact IFN-y production, receptor binding, and downstream signaling pathways, ultimately disrupting immune regulation. Loss-of-function mutations weaken the body's ability to combat infections such as tuberculosis and Salmonella, increasing the risk of chronic diseases such as Mendelian susceptibility to mycobacterial disease (MSMD). In contrast, gain-offunction mutations cause excessive IFN-y production, triggering chronic inflammation linked to autoimmune disorders (lupus and rheumatoid arthritis). Some mutations impair IFN-y receptor interactions, leading to immunodeficiency. In cancer, IFN-y mutations can either suppress tumor growth or contribute to chronic inflammation, promoting cancer progression. Understanding these genetic changes is essential for developing targeted treatments for infectious, autoimmune, and cancer-related conditions. The present study is to systematically analyse and predict the impact of

missense SNPs in the human IFN- γ gene using a comprehensive array of computational tools. By assessing the functional and structural consequences of these genetic variations, this study aims to identify potentially deleterious mutations that may influence immune regulation and disease susceptibility. The findings will contribute to a deeper understanding of IFN- γ -associated genetic variations and their role in infectious diseases, autoimmune disorders, and cancer, ultimately aiding in the development of targeted therapeutic strategies.

Materials and Methods

Collection and functional characterization of variants

The FASTA sequence of the human IFN-γ gene (NC000012 12) was retrieved from the NCBI database, with its corresponding UniProt ID P01579. Additionally, SNP data for IFN-y were obtained from the dbSNP-NCBI database for further computational analysis. Several bioinformatics tools were utilized to evaluate the potential functional consequences of variants. SNPnexus integrates multiple predictive algorithms, including SIFT and PolyPhen. SIFT classifies variants as tolerated or deleterious, with a threshold score of <0.05 indicating a deleterious effect (Fareed et al., 2022; Hasnain et al., 2020; Abdul Azeez, S., Borgio, 2016; Sim et al., 2012). PolyPhen evaluates variants as benign, possibly damaging, or probably damaging, with scores ranging from 0 to 1, where values closer to 1 indicate a higher likelihood of a damaging effect (Hasnain et al., 2020; Mahmud et al., 2016; Jahandideh and Zhi, 2014). The Protein Variation Effect Analyzer (PROVEAN) predicts the impact of amino acid substitutions or indels on protein function using sequence clustering and alignment-based scoring. Variants with a score below -2.5 are classified as deleterious, while those above this threshold are considered neutral (Fareed et al., 2022; Mahmud et al., 2016; Choi et al., 2012). Polymorphism Phenotyping v2 (PolyPhen-2) utilizes physical properties and comparative evolutionary analysis to classify variants as benign, possibly damaging, or probably damaging (Adzhubei et al., 2013). Consensus DELeteriousness (CONDEL) integrates the results of multiple predictive algorithms to assess the impact of singlenucleotide variants on protein function. It provides a consensus score, improving the accuracy of deleteriousness predictions (Gnad et al., 2013).

Assessment of variants for disease linkages and protein stability

The SNP and GO tool is used for predicting disease-associated amino acid changes in protein by utilizing the UniProt accession number and variant position to classify variants, with probability values >0.5 indicating disease-associated SNPs (Fareed et al., 2022; Hasnain et al., 2020; AbdulAzeez and Borgio, 2016; Magesh and George Priya Doss, 2014). P-MUT assesses the pathological impact of single amino acid variants in human proteins, achieving approximately 80% accuracy (López-Ferrando et al., 2017). PhD-SNP with a 78% accuracy rate, predicts disease-associated SNPs by ranking them on a scale of 0 to 9, to enhance the reliability of SNP classification through computational analysis. Meta-SNP predicts the impact of nsSNVs on protein function by integrating multiple tools. It assigns a score from 0 to 1, where values above 0.5 indicate disease-associated mutations (Fareed et al., 2022; Hasnain et al., 2020; Arshad et al., 2018; Jahandideh, S., Zhi; 2014; Magesh and George Priya Doss, 2014). The impact of mutations on protein stability can be assessed by analyzing changes in free

energy. I-Mutant 2.0 predicts stability changes due to nsSNPs with 77% accuracy, providing a reliability index (RI) from 0 to 10 (Fareed et al., 2022; Hasnain et al., 2020; Capriotti et al., 2006).

Secondary structure and solvent accessibility analysis

The Self-Optimized Prediction Method with Alignment (SOPMA) tool that predicts protein secondary structures by analyzing amino acid sequences (Santhoshkumar and Yusuf, 2020). It identifies regions likely to form α -helices, β -sheets, turns, or coils, offering insights into protein architecture. SOPMA enhances prediction accuracy by incorporating information from multiple sequence alignments of homologous proteins (Angamuthu and Piramanayagam, 2017; Geourjon, C., Deleage, 1995). NetSurfP-2.0 predicts key structural features of proteins, such as solvent accessibility, secondary structure, disorder regions, and backbone dihedral angles, by analyzing their amino acid sequences. It utilizes a combination of convolutional and bi-directional long short-term memory neural networks trained on solved protein structures. By inputting a protein sequence, researchers can obtain detailed insights into its structural characteristics, which are essential for understanding interaction interfaces and functional regions within the fully folded protein (Khan et al., 2021).

Structure prediction of IFN- y

The Protein Data Bank (PDB) entries for IFN-y structures, such as 1HIG and 1EKU, represent truncated versions of the protein, each consisting of 143 amino acids. These truncated forms were utilized to facilitate crystallization and structural analysis. Currently, no PDB structure encompasses the full-length 166 amino acid sequence of the IFN-y protein. Computational tools were employed to model the full-length IFN-y protein to achieve accurate structural predictions and analyses. AlphaFold was utilized to predict the three-dimensional coordinates of all heavy atoms in the protein based solely on its primary amino acid sequence (Jumper et al., 2021). The resulting structure was visualized using PyMOL, which simplified the depiction of the 3D conformation and allowed for the introduction of specific amino acid mutations. To enhance the accuracy of these models (30). ModRefiner was employed for structural refinement (Xu and Zhang, 2011). The quality of the refined models was assessed using the SAVES server, incorporating tools such as PROCHECK to generate Ramachandran plots that evaluate the stereochemical quality of the protein structures; a high percentage of residues in favored regions indicates good structural quality (Mahmud et al., 2016; Colovos and Yeates, 1993). Finally, TM-align was used to compare native and mutated protein structures, calculating metrics such as the TM-score and root-mean-square deviation (RMSD); a TM-score closer to 1 signifies high structural similarity, while a higher RMSD indicates greater differences between structures. Collectively, these computational approaches provide a comprehensive framework for modeling, refining, validating, and comparing protein structures, offering valuable insights into the structural and functional implications of IFN-y and its variants (Zhang and Skolnick. 2005; Zhang and Skolnick, 2004; Carugo and Pongor, 2001).

Virtual screening and molecular docking

To determine which of the listed compounds could potentially modulate the IFN-γ gene through molecular docking, a comprehensive computational analysis is required.

The 3D structures of the compounds can be sourced from PubChem, DrugBank, or ZINC database. Molecular docking studies using PyRx can then assess the binding affinity of these compounds to IFN-γ, providing insights into their potential interactions (Dallakyan and Olson, 2014; Trott, O., Olson, 2010; Morris et al., 2008). Among the listed compounds, S-Adenosylmethionine is known to regulate immune responses and cytokine expression, suggesting a possible role in IFN-γ modulation. Statins, including Simvastatin and Atorvastatin, have been reported to suppress IFN-γ-mediated inflammation, making them relevant candidates. Tamoxifen is commonly used in cancer therapy and may influence IFN-γ signaling pathways. Tetracycline, with its anti-inflammatory properties, could also affect IFN-γ expression. Additionally, COX-2 inhibitors such as Parecoxib and Rofecoxib are known to modulate immune responses, which may indirectly impact IFN-γ levels. To confirm their potential as IFN-γ modulators, further molecular docking and interaction studies are needed, analyzing parameters such as binding energy, hydrogen bonding, and hydrophobic interactions using Discovery Studio (Adeniji et al., 2020).

Results and Discussion

Variants collection

The human IFN-γ gene contains a total of 3,419 single-nucleotide polymorphisms (SNPs), and the corresponding protein sequences were retrieved from the NCBI database and analyzed using various computational algorithms. Among these SNPs, 77 were identified as non-synonymous SNPs (nsSNPs) affecting the IFN-γ protein. Additionally, the dataset included SNPs located in different regions: 146 in the untranslated regions (UTRs), 42 synonymous, 98 in the 5' upstream region, 1707 in non-coding regions, 919 in coding regions, and 58 in the 3' downstream region (*Figure I*). For further investigation, the identified nsSNPs in the IFN-γ protein were selected to assess their potential effects on protein structure, stability, and functional activity.

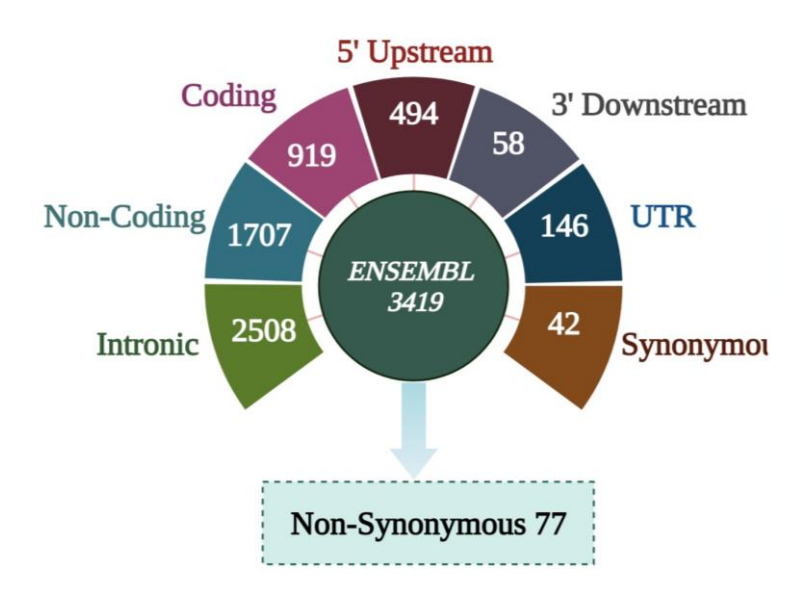


Figure 1. Outcome of SNPnexus server.

Download functionality detrimental variants

SNPnexus identified a total of 1,891 SNPs within the IFN-γ gene, each assigned a unique index. Using the SIFT algorithm, 26 non-synonymous SNPs (nsSNPs) were predicted to be deleterious, while 44 were considered tolerated (Figure 2). Further analysis with the PolyPhen-2 tool revealed 12 nsSNPs as probably damaging, 11 as possibly damaging, and 47 as benign. PolyPhen-2 scores range from 0 to 1, with values closer to 1 indicating higher potential for functional damage and values near 0 representing a likely benign impact. Additionally, a confidence score between 0 and 0.02 was assigned to 12 nsSNPs, while 9 nsSNPs with a score of 0 were classified as highly deleterious (Table 1). Among these, 12 variants G161R (rs769209772), R152Q (rs377736305), R130C (rs755519988), K78T (rs761801101), Y76F (rs867244009), (rs1009245499), **I72T** (rs56466653). 172N (rs56466653). V45E (rs1304053808), D114Y (rs1178805738), Y37C (rs1477303678), and A164S (rs369578383) were consistently predicted to be harmful by both SIFT and PolyPhen. These missense SNPs were further validated through comprehensive analysis using additional in silico tools, including PPh2, PROVEAN and ConDEL (Table 1). Additionally, PROVEAN analysis identified 10 nsSNPs in the human IFN-y gene as deleterious, whereas M1L (-1.921) and A164S (-0.856) were predicted to be neutral (Table 1). Moreover, I72T, R130C, and Y37C exhibited the most damaging effects, with PROVEAN scores of -6.410, -6.301, and -6.158, respectively. According to PolyPhen-2 (PPh2), 11 nsSNPs were predicted to be probably damaging to the IFN-γ protein, with scores ranging from 0.818 to 1.000. The A164S variant was considered possibly damaging, with a score of 0.818. Furthermore, ConDEL uses a consensus weighted scoring approach, classifying 9 nsSNPs as deleterious and G161R, M1L, and A164S as neutral. The comprehensive functional deleterious consequences of these nsSNPs are detailed in Table 1.

Table 1. List of deleterious IFN-γ variations found by SIFT> PolyPhen>PROVEAN>PPh2 and ConDEL algorithms.

rs ID	Sub	SII	T	PolyP:	hen	PRC	VEAN	P	Ph2	ConDE	EL
		S	Е	S	Е	S	Е	S	Е	S	Е
rs769209772	G→R 161	0	D	0.923	PD	D	-3.04	PD	0.992	0.471646	N
rs377736305	R→Q 152	0	D	0.967	PD	D	-2.63	PD	1	0.584477	D
rs755519988	R→C 130	0	D	0.995	PD	D	-6.301	PD	1	0.588284	D
rs761801101	$K \rightarrow T78$	0	D	0.984	PD	D	-4.615	PD	0.999	0.577837	D
rs867244009	Y→F 76	0	D	0.998	PD	D	-3.63	PD	1	0.656726	D
rs564666653	I→T 72	0	D	0.992	PD	D	-4.52	PD	0.998	0.613629	D
rs56466653	I→N 72	0	D	0.997	PD	D	-6.41	PD	1	0.614522	D
rs1009245499	V→E 45	0	D	0.963	PD	D	-4.324	PD	0.996	0.594845	D
rs1304053808	$M\rightarrow L 1$	0	D	0.956	PD	D	-1.921	PD	0.984	0.33308	N
rs1178805738	D→Y 114	0.01	D	0.987	PD	D	-4.244	PD	1	0.576615	D
rs1477303678	Y→C 37	0.01	D	0.991	PD	D	-6.158	PD	1	0.584235	D
rs369578383	A→S 164	0.02	D	0.991	PD	D	-0.856	Pos	0.818	0.442043	N

Note: Sub=Substitutions; D=Deleterious; E=Effect; N=Neutral; S=Score; PD=Probably Damaging; Pos=Possibly Damaging.

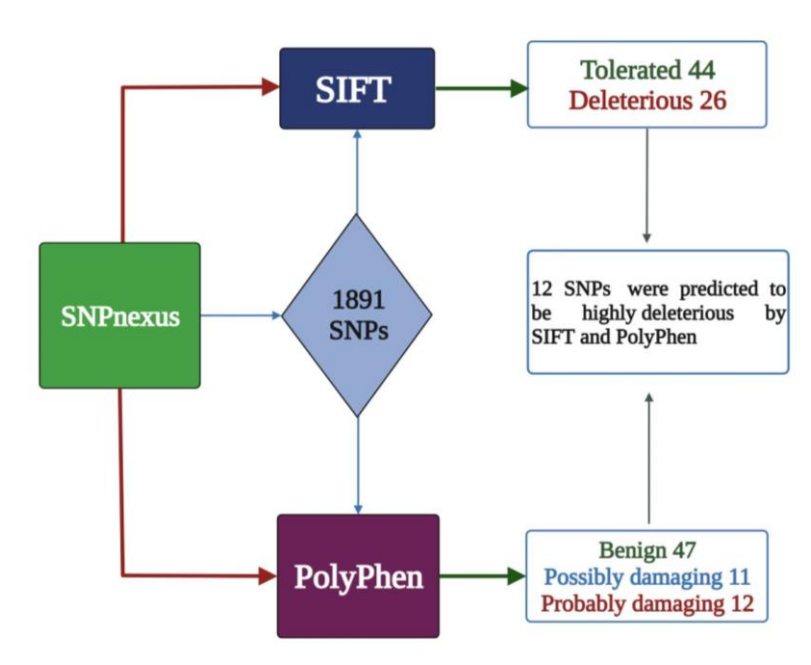


Figure 2. Findings of SIFT and PolyPhen algorithms.

Evaluating disease prediction and effect on stability

SNP and GO determined that 8 missense variants were classified as disease-causing, while G161R, M1L, D114Y, and A164S were predicted to be neutral. In contrast, P-Mut predicted only G161R, R152Q, K78T, D114Y, Y37C, and A164S as false positives, indicating possible disease variations. Similarly, PhD-SNP categorized G161R, M1L, D114Y, and A164S missense variants as neutral and the remaining eight as disease-causing (*Table 2*). Meta-SNP predicted five nsSNPs as having damaging effects on the IFN-γ protein (*Table 2*). To further assess protein stability, I-Mutant was used to evaluate single-site mutations and predicted that K78T, Y76F, and Y37C significantly reduced protein stability, with the corresponding Reliability Index (RI) values (*Table 2*). These polymorphisms were identified as the most detrimental, likely due to their strong destabilizing effects on the IFN-γ protein structure.

Table 2. Forecasting functional nsSNPs associated with disease and the impact on protein stability.

rs ID	Sub	P-Mu	SNP&	GO	PhD	-SNP	Meta	a SNP	I-Mut	ant
		Е	S	Е	Е	S	Е	S	Е	RI
rs769209772	G→R 161	F	0.4901	N	N	3	N	6		3
rs377736305	R→Q 152	F	0.3049	D	D	0	N	3	\downarrow	7
rs755519988	R→C 130	T	0.6878	D	D	6	D	4	\downarrow	6
rs761801101	$K \rightarrow T78$	F	0.4397	D	D	3	N	5	1	1
rs867244009	Y→F 76	T	0.5444	D	D	2	N	0	1	3
rs56466653	I→T 72	T	0.632	D	D	4	D	0	\downarrow	8
rs56466653	I→N 72	T	0.7265	D	D	5	D	5	\downarrow	6
rs1009245499	V→E 45	T	0.6811	D	D	6	D	4	\downarrow	9
rs1304053808	$M\rightarrow L 1$	T	0.7101	N	N	6	N	5	ļ	4
rs1178805738	D→Y 114	F	0.4585	N	N	0	N	1	1	6
rs1477303678	Y→C 37	F	0.4691	D	D	4	D	2	†	3
rs369578383	A→S 164	F	0.3771	N	N	9	N	8	Į.	8

Note: Sub=Substitutions; D=Disease; E=Effect; F=False; N=Neutral; S=Score; T=True; \downarrow =Decrease; \uparrow =Increase.

Secondary structure and solvent accessibility

The SOPMA secondary structure prediction revealed that the protein predominantly consists of alpha helices, which account for 66.27% (110 residues) of the structure. Extended strands make up 5.42% (9 residues), beta turns comprise 1.20% (2 residues), and random coils constitute 27.11% (45 residues). No residues were found in 310 helices, π -helices, beta bridges, or bend regions (*Figure 3*). The analysis was performed using a window width of 17, a similarity threshold of 8, and involved four defined structural states. This indicates a highly helical structure with moderate flexibility suggested by the presence of random coils. This predominance of α -helical regions over β-sheet structures reflects its essential role in maintaining conformational resilience, which is critical for the protein's functional performance in immune signaling pathways. Moreover, NetSurfP analysis highlighted the solvent accessibility and structural disorder of several missense variants. Notably, high disorder scores were observed for G161R (99%), R152Q (98%), M1L (97%), and A164S (99%), while Y37C showed moderate disorder (29%), and V45E exhibited a solvent accessibility of 55%. The wildtype residues for all variants were found to be buried (Figure 4). The analysis was based on 166 residue predictions from a single sequence, with a processing time of 130 seconds (Figure 5). Among the variants, G161R (rs769209772) showed RSA 72% and ASA 57%; R152Q (rs377736305) had RSA 73% and ASA 167%; R130C (rs755519988) showed RSA 53% and ASA 119%; K78T (rs761801101) had RSA 47% and ASA 97%; and Y76F (rs867244009) had RSA 9% and ASA 20%. The I72T and I72N mutations (rs564666653) both had RSA 5% and ASA 9%. V45E (rs1009245499) exhibited RSA 33% and ASA 51%; M1L (rs1304053808) showed RSA 72% and ASA 144%; D114Y (rs1178805738) had RSA 37% and ASA 53%; Y37C (rs1477303678) had RSA 40% and ASA 86%; and A164S (rs369578383) showed RSA 74% and ASA 81%. Overall, NetSurfP provided insight into the burial or exposure of residues, with RSA reflecting the proportion of solvent exposure relative to the maximum possible, and ASA indicating the absolute accessible surface area of each residue.

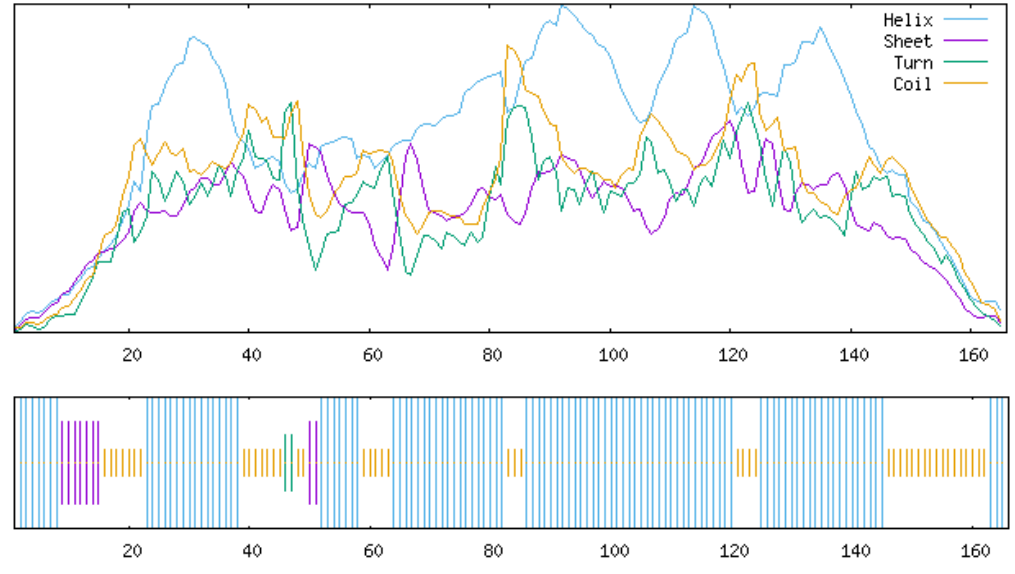


Figure 3. SOPMA prediction results for the IFN-y protein.

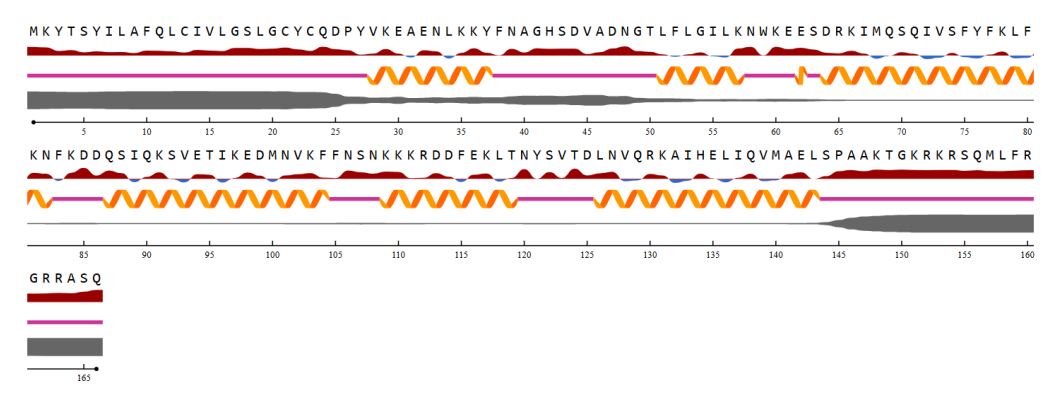


Figure 4. NetSurfP3 server examines the disorder, surface accessibility, and dihedral angles of the IFN-γ sequence.

Homology modeling and quality prediction

Protein structure prediction is essential for interpreting protein bioactivity, and the 3D structure of IFN-γ was modeled using Alphafold (Figure 4). The model was subsequently refined using ModRefiner, which improved its structural quality and stability. The ERRAT analysis of the predicted protein indicated a quality factor of 95.2381% based on the sliding 9-residue window, confirming a high-resolution and reliable model. Additionally, the 3D Verify tool assessed the structure and indicated that 48.19% of the amino acids exhibited a quality score of 0.2 or better in the 3D-1D profile. The Ramachandran plot analysis of the native IFN-γ protein using PROCHECK revealed that 95.50% of residues are in the core region, 4.50% in the allowed region, and 0.00% in both the generously allowed and disallowed regions, indicating a highquality and stereochemically stable structure (Figure 5). The QMEAN4 value of the refined model was -1.87, indicating a reasonably good model quality (Figure 5). Mutants K78T (rs761801101), Y37C (rs1477303678), and Y76F (rs867244009) exhibited higher RMSD values of 0.55, 0.61, and 0.59, respectively (Figure 5), prompting molecular docking analysis. The complete structural validation results are summarized in Table 3.

Table 3. Structural validation analysis of IFN-y protein.

Table 5. Structural validation analysis of IFN-y prolein.									
rs ID	Sub	ERRAT	3D verify		Pro cl	heck		TM a	lign
				С	A	G	D	T	R
IFN-γ		95.2381	48.19%	95.50%	4.50%	0.00%	0.00%	-	
rs769209772	G→R 161	95.1049	56.02%	94.80%	3.69%	0.00%	0.00%	0.98027	0.43
rs377736305	$R \rightarrow Q 152$	95.2703	52.41%	94.80%	4.50%	0.60%	0.00%	0.99048	0.49
rs755519988	R→C 130	97.9167	49.40%	96.10%	3.20%	0.60%	0.00%	0.99029	0.49
rs761801101	$K \rightarrow T78$	96.6216	51.81%	96.10%	3.20%	0.60%	0.00%	0.98802	0.55
rs867244009	Y→F 76	97.9592	50.60%	94.20%	5.80%	0.00%	0.00%	0.98709	0.59
rs564666653	I→T 72	96.6216	43.37%	97.40%	2.60%	0.00%	0.00%	0.99204	0.44
rs564666653	I→N 72	94.4444	45.18%	95.50%	4.50%	0.00%	0.00%	0.98851	0.53
rs1009245499	V→E 45	94.7368	40.36%	95.50%	4.50%	0.00%	0.00%	0.99223	0.43
rs1304053808	$M\rightarrow L 1$	95.1049	56.02%	94.34%	3.20%	0.00%	0.00%	0.96841	0.44
rs1178805738	D→Y 114	94.4564	43.67%	93.56%	2.60%	0.00%	0.00%	0.96852	0.49
rs1477303678	Y→C 37	98.6207	44.58%	95.50%	4.50%	0.00%	0.00%	0.98575	0.61
rs369578383	A→S 164	94.5609	49.54%	95.50%	3.50%	0.01%	0.00%	0.98853	0.45

Note: Sub=Substitutions; C=Core; A=Allowed; G=Generously; D=Disallowed; T=TM Score; R=RMSD.

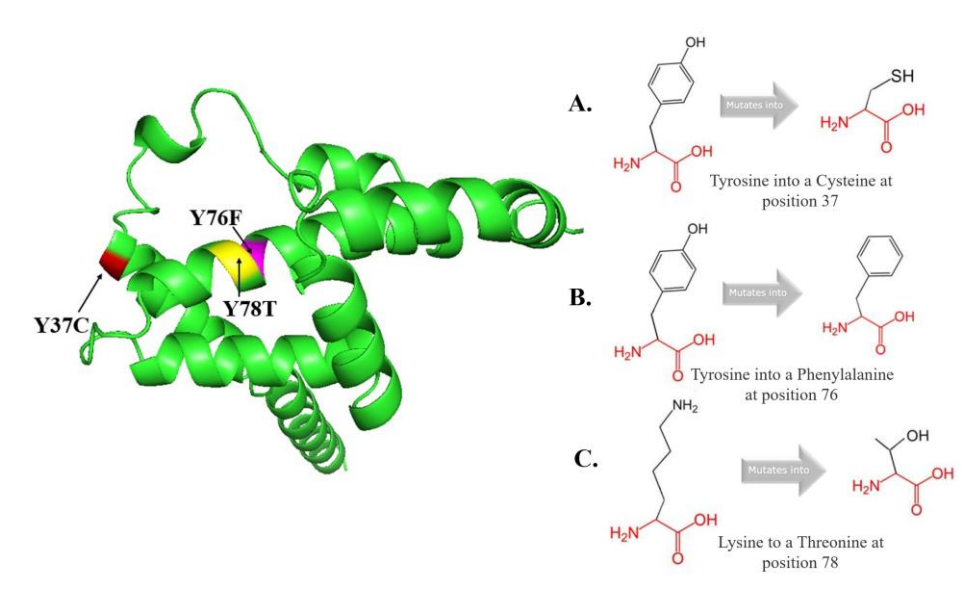


Figure 4. Tertiary structure of IFN-y mutant protein.

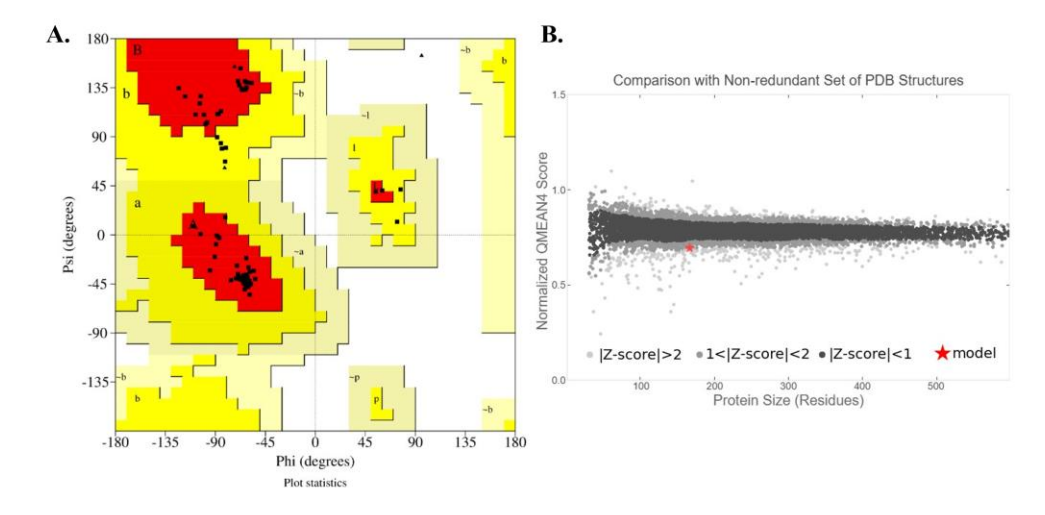


Figure 5. Procheck-RAMACHANDRAN Plot of IFN-y and QMEAN analysis.

Protein ligand visual screening

Molecular docking studies are essential for understanding protein-ligand interactions, identifying active compounds, interpreting molecular mechanisms, and facilitating drug discovery and design. In this study, PyRx AutoDock Vina was employed to estimate the binding affinities between ligands and the target protein. A grid box of appropriate dimensions was centered on the coordinates of the crystal structure to accurately define the active site of the target protein. To further analyze the predicted protein-ligand interactions, Discovery Studio was used for visualization and interpretation. A total of 25 top-ranking compounds were retrieved from the PubChem and ZINC databases, exhibiting binding free energies ranging from –2.7 to –8.8 kcal/mol (*Table 4*). These ligands demonstrated significant interactions with both the wild-type IFN-γ protein and its mutant forms (Y37C, K78T, and Y76F), suggesting their potential as promising drug candidates. The 2D interaction diagrams generated in Discovery Studio illustrated

specific interactions between ligand atoms and key residues within the active site of IFN-γ (Figure 6). In particular, the dotted lines in the diagram indicate hydrogen bonds and other interactions formed between the ligands and the residues of the wild-type protein. The molecular docking analysis of various ligands, Laminin, Tamoxifen, JMS, FUL (Fulvestrant), Melanin, Parecoxib, and Rofecoxib, against IFN-γ and Y37C, K78T, and Y76F revealed significant differences in binding affinities and interaction profiles. Among all ligands, Laminin exhibited the strongest binding affinity with the native IFN-γ protein (-8.8 kcal/mol), involving crucial interactions with residues such as Leu118, Lys117, Phe105, Val73, and Phe115 through Van der Waals forces, Pi-Pi stacking, and alkyl interactions. These strong interactions were preserved across Y37C, K78T, and Y76F, with only slight variations in binding energies (-8.4 to -8.7 kcal/mol), indicating Laminin's robust binding capacity irrespective of point mutations. Tamoxifen also showed a high binding affinity (-8.5 kcal/mol) with the native IFN-γ, forming hydrogen bonds (notably with Glu116) and engaging in Pi-alkyl interactions with Phe77 and Val73. However, its interaction with the mutant forms was not elaborated in detail. FUL demonstrated moderate binding affinity (-7.4 kcal/mol with native and -7.0 kcal/mol with mutants), forming conventional hydrogen bonds and maintaining interactions mainly with Phe115, Glu116, Lys78, and surrounding residues (*Table 5*).

Table 4. Docking score (-Kcal/mol) outcomes of IFN-γ, Y37C, Y76F and K78T nsSNPs with 25 ligands.

Ligands	IFN-γ	Y37C	Y76F	K78T
BCT	-2.7	-2.3	-2.4	-2.6
FUL	-7.4	-7	-6.9	-7
GLC	-4.3	-4.2	-4.1	-4.1
GOL	-3.2	-3.2	-3.1	-3.1
INS	-2.4	-1.9	-1.8	-1.9
IU1	-6.8	-5.3	-5.8	-6.2
JMS	-6.9	-6.2	-6.2	-6.1
Laminin	-8.8	-8	-8.7	-8.1
Lomiflaxcin	-6.6	-6.6	-6.3	-6.5
M2P	-4.4	-4.8	-4.8	-4.9
Melanin	-7.2	-7.7	-7.2	-7.7
Memantine	-6.1	-5.4	-5.4	-5.4
MPD	-4.6	-3.7	-3.3	-3.5
OXL	-3.3	-3.1	-2.9	-2.8
Parecoxib	-6.9	-7	-7.6	-7.8
PFN	-2.3	-1.9	-1.9	-2
Pirnixic Acid	-5.6	-5.6	-6.1	-6.1
Rofecoxib	-6.9	-6.7	-6.6	-6.5
S-Adenosylmethionine	-5.1	-6	-6.4	-5.3
Statin	-6	-5	-4.7	-4.9
Tamoxifen	-8.5	-6.5	-6.5	-6.5
Tetracycline	-6.6	-6.4	-6.5	-6.5
TVY	-5.6	-5.3	-5.8	-5.4
Z8T	-5	-4.6	-3.9	-4
Zanamivir	-4.8	-5.2	-5.7	-5

Table 5. Molecular docking interaction of ligands with wild type (WT) and mutant forms of $IFN-\gamma$ protein.

Protein type	Ligand	Hydrophilic interaction (residue)	Additional hydrophilic interaction
WT	Laminin	Leu118, Lys117, Asn120, Lys78, Phe75,	Phe115, Val73, Phe47, Glu116, Thr119,
		Tyr76, Ser70, Ile72, Phe105, Lys97	Ser74
WT	FUL	Phe115, Lys78, Asn120, Glu116, Val73,	Phe77, Thr119
		Ser74	
WT	Melanin	Lys97, Arg112, Glu116, Tyr121, Leu118,	Phe115, Ser74, Val73, Phe77, Thr119,
		Phe105, Met100, Ile72, Phe75, Lys78,	Asn120
		Lys81, Tyr76	
WT	JMS	Lys78, Tyr76, Phe104, Phe80, Lys97,	Glu116, Phe77, Val73, Met100, Thr119,
		Phe115, Tyr121, Lys117, Ser74	Asn120
WT	Rofecoxib	Lys117, Thr121, Leu118, Lys81, Lys97,	Phe77, Val73, Glu116, Asn120, Thr119,

eISSN: 2785-8243

		Phe115, Arg112, Phe105, Tyr76, Ile72, Phe75, Lys78	Ser74
WT	Tamoxifen	Phe105, Lys97, Phe80, Phe75, Lys70, Lys81, Tyr121, Lys117, Glu116	Val180, Val210, Val73, Ser74, Phe77, Thr119, Asn120, Ile72, Tyr76
Y37C	Laminin	Lys117, Leu118, Asn120, Lys78, Phe75, Tyr76, Ser70, Ile72, Phe105, Lys97	Phe115, Glu116, Thr119, Phe77, Val73, Ser74
Y37C	FUL	Asn120, Phe105, Val73, Lys78, Glu116, Ser74	Thr119, Phe77, Phe115
Y37C	Lomifloxacin	Phe115, Lys78, Phe105, Ser74, Tyr76, Phe104, Lys97, Phe80, Lys117, Tyr121, Leu118, Glu116, Met100	Lys81, Asn120, Thr119, Val93, Phe77
Y37C	Melanin	Leu118, Tyr121, Lys117, Phe80, Lys97, Phe104, Tyr76, Ser74, Phe105, Lys78, Phe115, Glu116, Met100	Phe77, Lys81, Asn120, Thr119, Val73
Y37C	Parecoxib	Lys117, Phe115, Met100, Phe105, Lys97, Tyr76, Ile72	Lys78, Asn120, Glu116, Thr119, Phe77, Val73, Ser74, Phe75
Y37C	Rofecoxib	Leu118, Lys81, Lys97, Arg112, Phe105, Tyr76, Ile72, Phe75, Lys78, Lys117, Tyr121	Phe77, Val73, Glu116, Asn120, Thr119, Ser74
Y76F	FUL	Lys78, Phe75, Thr119, Asn120, Lys117, Leu118, Phe105	Val73, Ser74, Phe77, Phe115, Glu116
Y76F	Laminin	Ile72, Phe75, Lys78, Met100, Phe105, Lys47, Arg112, Glu116, Tyr121, Leu118, Lys81, Phe76	Phe115, Ser74, Val73, Phe77, Thr119, Asn120
Y76F	Melanin	Glu116, Phe115, Lys78, Phe105, Ser74, Phe76, Phe104, Phe80, Lys97, Lys117, Tyr121, Leu118, Met100	Phe77, Lys81, Asn120, Thr119, Val73
Y76F	Parecoxib	Lys97, Phe76, Ile72, Lys117, Phe115, Met100, Phe105	Thr119, Asn120, Glu116, Phe71, Val73, Ser74, Phe75, Lys78
Y76F	Rofecoxib	Leu118, Lys81, Lys97, Arg112, Phe105, Phe76, Ile72, Phe75, Lys78, Lys117, Tyr121	Glu116, Asn120, Thr119, Phe77, Val73, Ser74
Y76F	Tamoxifen	Phe105, Lys97, Phe80, Phe75, Lys70, Lys81, Tyr121, Lys117, Glu116	Val180, Val210, Val73, Ser74, Phe77, Tyr76, Ile72, Phe115, Thr119, Asn120
K78T	FUL	Phe75, Thr78, Thr119, Asn120, Lys117, Leu118, Phe105	Val73, Phe77, Ser74, Phe115, Glu116
K78T	Laminin	Lys97, Lys117, Phe105, Ile72, Ser70, Tyr76, Tyr78, Asn120, Leu118	Phe115, Val73, Phe77, Thr119, Glu116, Ser74
K78T	Melanin	Glu116, Phe115, Thr78, Ser74, Phe105, Tyr76, Phe104, Lys97, Phe80, Lys117, Thr121, Leu118, Met100	Phe77, Lys81, Asn120, Thr119, Val73
K78T	Parecoxib	Lys97, Tyr76, Ile72, Phe105, Met100, Phe115, Lys117	Thr78, Thr119, Asn120, Glu116, Phe77, Val73, Ser74, Phe75
K78T	Rofecoxib	Leu118, Lys81, Lys97, Phe115, Arg112, Phe105, Tyr76, Ile72, Phe75, Thr78, Lys117, Tyr121	Phe77, Val73, Asn120, Thr119, Ser74, Glu116

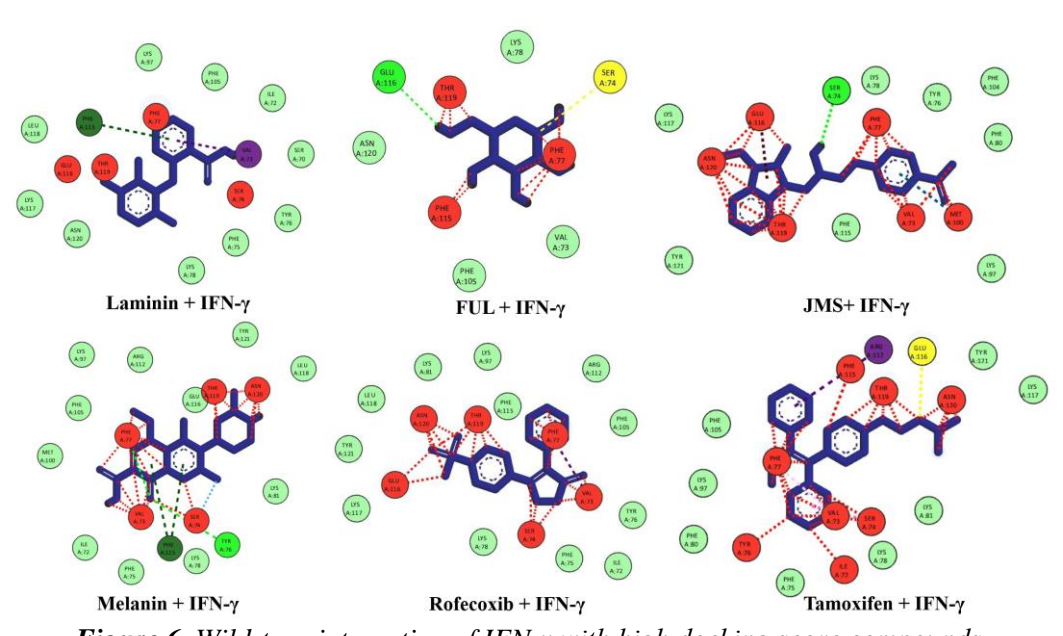


Figure 6. Wild-type interaction of IFN-γ with high docking score compounds.

Melanin showed an enhanced binding affinity in the mutant forms (-7.7 kcal/mol) compared to the IFN-y (-7.2 kcal/mol), with key involvement of residues Arg112, Phe105, Phe77, and Glu116 (Table 5). These interactions included Pi-Pi stacking and hydrogen bonds, suggesting Melanin may bind more effectively to mutant IFN-y than the native protein. Parecoxib and Rofecoxib exhibited comparatively lower binding affinities. Parecoxib had a binding score of -6.9 kcal/mol with the native form, which slightly improved to -7.8 kcal/mol in the K78T and Y76F mutants. Key interactions included hydrogen bonding and Pi-alkyl interactions with Phe115, Lys117, and Met100. Similarly, Rofecoxib showed a binding affinity of -6.9 kcal/mol with the native IFN-y, which decreased slightly in the mutant proteins (-6.5 kcal/mol), though core interactions with residues such as Tyr76, Arg112, Val73, and Phe105 remained conserved (*Table 5*). Overall, the analysis revealed that Laminin and Melanin maintain strong and consistent interactions with both native and mutant IFN-y proteins, indicating their potential as stable therapeutic binders. Meanwhile, FUL, Parecoxib, and Rofecoxib demonstrated variable interaction profiles and reduced binding strengths. Across all docking studies, critical interacting residues consistently included Phe115, Glu116, Phe105, Val73, Ser74, and Phe77, which appear to play central roles in ligand stabilization (Table 5). These findings suggest that specific mutations in IFN-y do not drastically alter its binding pocket, allowing certain ligands to retain their efficacy. The ligands analyzed in this study laminin, tamoxifen, fulvestrant (FUL), melanin, parecoxib, and Rofecoxib show promising potential in the treatment of IFN-y-related disorders. IFN-y is a crucial cytokine involved in immune system regulation, primarily responsible for macrophage activation, antigen presentation, and the coordination of adaptive immune responses. Dysregulation or mutations in the IFN-γ gene are associated with several immunerelated disorders, such as autoimmune diseases, chronic inflammation, and Mendelian susceptibility to mycobacterial diseases (MSMD). The molecular docking results demonstrated strong binding affinities of laminin and melanin, with both wild-type and mutant IFN-y proteins. These interactions suggest that these ligands could help stabilize the mutated protein, restore its normal function, or modulate its activity to balance immune responses.

These compounds also play an essential role in future structure-based drug discovery. The favorable interactions of ligands such as laminin and melanin with critical amino acid residues (Phe115, Glu116, Phe105, and Val73) across all IFN-y variants indicate their potential as lead molecules. Their consistent binding in both wildtype and mutant forms highlights their capacity to function as broad-spectrum therapeutic agents, capable of targeting a range of IFN-y-related dysfunctions. Moreover, tamoxifen and fulvestrant are estrogen receptor modulators, and antiinflammatory drugs like parecoxib and rofecoxib, may offer repurposing opportunities for immunomodulatory treatment, potentially enhancing the efficacy of therapies targeting chronic inflammation and immune imbalance. Despite these promising findings, the study has several limitations. First, the analysis is purely computational; hence, the predicted interactions require experimental validation through in vitro assays, animal studies, and clinical trials to confirm biological relevance, safety, and effectiveness. Second, the study only examined Y37C, K78T, and Y76F, while realworld patient populations may present with more diverse and complex mutations. Additionally, the primary pharmacological roles of tamoxifen, fulvestrant, and other ligands might pose challenges due to off-target effects or toxicities if repurposed without structural optimization. However, this study opens possibilities for drug repurposing, using clinically approved compounds, and supports rational drug design. It also advances precision medicine by tailoring treatments to genetic profiles, enhancing therapeutic outcomes. However, further validation through experimental studies is needed to fully assess the biological significance of these predictions.

Interferon-gamma (IFN-γ) is a critical regulator of tumor progression and immunemediated tumor suppression. It is predominantly expressed by antigen-activated T cells, natural killer (NK) cells, natural killer T (NKT) cells, and dendritic cells. The term "interferon" (IFN) was first introduced in 1957 following the discovery of a factor capable of inhibiting influenza virus replication in murine models. (1) This discovery led to the identification of a novel family of cytokines known as interferons (IFNs), which are categorized into three major types: Type I (IFN-α), Type II (represented solely by IFN-γ), and Type III (IFN-λ), comprising IFN-λ1, IFN-λ2, and IFN-λ3 formerly designated as IL-28A, IL-28B, and IL-29. (2) Type I IFN genes are conserved across all vertebrate species. Among them, 13 IFN-α genes encode 12 structurally identical IFN-α protein isoforms. In amphibians, IFN genes exhibit structural diversity, as they may exist either as intronless sequences or contain introns, reflecting evolutionary variability in gene organization. (3-5). A distinctive feature of IFN-y is its conserved C-terminal tail, which is maintained across a wide range of species, including fish, amphibians, birds and mammals. This conserved region is enriched with LYS and ARG residues, which are crucial for the protein integrity (8). Furthermore, IFN-y mutations also disrupt receptor interactions, resulting in immunodeficiency. In cancer, IFN-γ mutations can either suppress tumor growth or contribute to chronic inflammation that fosters cancer progression. Understanding these genetic alterations is crucial for developing targeted therapies for infectious diseases, autoimmune disorders, and cancer.

Genome-wide association studies (GWAS) have revealed multiple IFN-y polymorphisms associated with altered immune responses. These genetic variations can enhance susceptibility to a range of infectious diseases, autoimmune disorders, and inflammatory conditions by affecting the expression and function of the IFN-y gene (9). Moreover, data from the Catalogue of Somatic Mutations in Cancer (COSMIC) reveals that 49,967 unique samples were analysed, 243 exhibited mutations in the IFN-γ gene. These mutations can affect IFN-y production, receptor binding, and downstream signaling, ultimately disrupting immune regulation. Notably, the rs1861494 SNP has been associated with leprosy, asthma, and non-Hodgkin lymphoma, while the rs2069718 SNP has been linked to severe cases of COVID-19, suggesting its potential role in disease severity. Additionally, the rs2430561 SNP has been implicated in susceptibility to tuberculosis, underscoring its importance in immune response Loss-of-function mutations in the IFN-y gene impair the host's regulation (10). immunity to defend against tuberculosis and Bacterial infections, increasing the risk of Mendelian susceptibility to mycobacterial disease (MSMD). Gain-of-function mutations lead to excessive IFN-y production, which can induce chronic inflammation associated with lupus and rheumatoid arthritis.

The IFN- γ gene is located on human loci on 12q14.1 and spans roughly 9.6 kilobases, encompassing 4 exons and 3 introns. It encodes IFN- γ gene lies between base pairs 57,700,000 and 67,300,000 and is tightly regulated by promoter and untranslated regions (UTRs), which contain binding sites for key transcription factors such as STAT1, NF- κ B, and IRF-1. These regulatory elements modulate IFN- γ expression in response to immune stimuli, including infections and inflammatory signals. The IFN- γ

protein is initially synthesized as a monomer consisting of 146 amino acids, but following post-translational modifications, it forms a biologically active homodimer with 166 amino acids (6). Structurally, IFN- γ belongs to the type II IFN family and features a helical bundle composed of six α -helices (A–F), which are essential for binding to its receptor complex (IFNGR1 and IFNGR2) and initiating downstream immune signaling. The structural integrity and regulated expression of IFN- γ are fundamental to its role in orchestrating effective immune responses, and disruptions in its gene or protein structure can lead to immune-related disorders (7). This study focuses on the computational analysis of missense variants in the human IFN- γ gene that may disrupt protein function and contribute to immune-related disorders. By predicting the functional and structural effects of these variants, including secondary structure and solvent accessibility using SOPMA and NetSurfP, the research aims to uncover potentially damaging mutations. The outcomes are expected to provide valuable insights into the role of IFN- γ gene variations in infectious diseases, autoimmune conditions, and cancer, paving the method for the development of targeted therapeutic approaches.

Our findings showed that 1,891 SNPs within the IFN-y gene by the SNPnexus algorithm and G161R (rs769209772), R152Q (rs377736305), R130C (rs755519988), K78T (rs761801101), Y76F (rs867244009), I72T (rs564666653), I72N (rs564666653), V45E (rs1009245499), M1L (rs1304053808), D114Y (rs1178805738), (rs1477303678), and A164S (rs369578383) were predicted to be highly deleterious. Additionally, PROVEAN analysis identified 10 nsSNPs in the human IFN-y gene as deleterious, whereas M1L (-1.921) and A164S (-0.856) were predicted to be neutral. Furthermore, I72T, R130C, and Y37C exhibited the most damaging effects, with PROVEAN scores of -6.410, -6.301, and -6.158, respectively. ConDEL uses a consensus weighted scoring approach, classified 9 nsSNPs as deleterious and G161R, M1L, and A164S as neutral. According to PPh2, 11 nsSNPs were predicted to probably damage the IFN-y protein. ConDEL classified G161R, M1L, and A164S as neutral, while SNP and GO also predicted G161R, M1L, D114Y, and A164S as neutral variants. P-Mut identified G161R, R152Q, K78T, D114Y, Y37C, and A164S as false positives. PhD-SNP categorized four missense variants as neutral, whereas Meta-SNP predicted five nsSNPs as having damaging effects. Additionally, I-Mutant analysis revealed that K78T, Y76F, and Y37C significantly reduced protein stability. SOPMA analysis showed that IFN- γ is predominantly α -helical (66.27%), with minor contributions from extended strands (5.42%), beta turns (1.20%), and random coils (27.11%), indicating a stable yet moderately flexible structure. This helical dominance supports its structural integrity in immune signaling. NetSurfP analysis revealed high disorder in G161R (99%), R152Q (98%), M1L (97%), and A164S (99%), while Y37C showed moderate disorder (29%), and V45E had a solvent accessibility of 55%. All wild-type residues were buried, suggesting a structural impact upon mutation.

The 3D model generated by AlphaFold showed good quality, with 95.5% of residues in favored regions and a QMEAN4 score of -1.87. Mutants K78T, Y37C, and Y76F exhibited elevated RMSD values (0.55–0.61), demanding further docking analysis. Molecular docking studies revealed that Laminin exhibited the strongest binding affinity to both wild-type and mutant forms of IFN-γ, with a binding energy of -8.8 kcal/mol for the wild-type and similar affinities for the mutants (Y37C, K78T, Y76F). Melanin also showed enhanced binding to the mutant forms compared to the wild-type, suggesting its potential to bind more effectively in the presence of mutations. Tamoxifen and Fulvestrant displayed moderate binding affinities, with variable interaction profiles in

the mutant forms, while Parecoxib and Rofecoxib demonstrated lower binding strengths. These findings highlight Laminin and Melanin as promising candidates for stabilizing IFN-γ, potentially modulating immune responses in disorders related to IFN-γ dysfunction. The consistency of interactions with key residues (Phe115, Glu116, Phe105, and Val73) across wild-type and mutant proteins underscores their therapeutic potential. However, the results require experimental validation, and repurposing compounds like Tamoxifen and Fulvestrant may need structural optimization to reduce off-target effects and enhance their efficacy.

These findings offer valuable insights for drug discovery, particularly in targeting IFN-γ-related immune disorders. The identification of Laminin and Melanin as strong binders to both wild-type and mutant IFN-y proteins suggests their potential as therapeutic agents for stabilizing the protein or modulating its activity. This can be particularly beneficial in conditions where IFN-y dysfunction is involved, such as autoimmune diseases or chronic inflammation. Additionally, the fact that these ligands demonstrate consistent binding across various mutations indicates their broad-spectrum potential, which could be crucial for treating genetically diverse patient populations with IFN-γ-related disorders. The novelty of these findings lies in their application to mutant forms of IFN-y, an area that has not been extensively explored in prior drug discovery studies. While IFN-y role in immune regulation is well-established, targeting its mutant forms with specific ligands opens new avenues for precision medicine. Furthermore, repurposing existing compounds like Tamoxifen and Fulvestrant for IFNγ-related dysfunction is a novel approach that could expedite drug development by utilizing already-approved drugs for new therapeutic indications. This research thus paves the way for further experimental validation and optimizes the potential for therapeutic intervention in IFN-y-associated diseases.

Conclusion

The study provides significant insights into the genetic and structural implications of missense mutations in the IFN-y gene, with implications for immune-related disorders, cancer, and infectious diseases. Through computational analysis, 1,891 SNPs within the IFN-γ gene were evaluated, identifying several highly deleterious variants, including G161R, R152Q, R130C, K78T, Y76F, I72T, and others, which were predicted to disrupt protein function and stability. The analysis highlighted that I72T, R130C, and Y37C, exhibited the most damaging effects, potentially compromising immune signaling pathways essential for regulating immune responses. The molecular modeling and docking studies further emphasized the critical role of IFN-y's structural integrity, with identified ligands such as Laminin and Melanin showing strong binding affinities to both wild-type and mutant IFN-y proteins, suggesting their potential as therapeutic agents for stabilizing or modulating the protein's activity. Laminin and Melanin represent promising candidates for future drug development due to their ability to interact with key residues on both wild-type and mutant IFN-γ proteins, potentially offering a broad-spectrum therapeutic approach. Additionally, Tamoxifen and Fulvestrant could accelerate the clinical application of these compounds for IFN-yrelated dysfunctions, though further structural optimization may be needed. By targeting the structural and functional consequences of specific genetic variants, this research opens new avenues for precision medicine in treating IFN-y-related diseases. The results underline the potential of integrating computational drug discovery approaches with

existing pharmaceutical compounds, facilitating the rapid identification and validation of therapeutic candidates for a range of immune-mediated diseases. Future experimental validation of these findings will be essential for confirming their therapeutic potential and optimizing treatment strategies for individuals with IFN-y-related immune disorders.

Acknowledgement

The authors gratefully acknowledge the research staff and collaborators who contributed to the successful completion of this work.

Conflict of interest

The authors confirm that there is no conflict of interest involve with any parties in this research study.

REFERENCES

- AbdulAzeez, S., Borgio, J.F. (2016): In-silico computing of the most deleterious nsSNPs in HBA1 gene. – PloS One 11(1): 13p.
- [2] Adeniji, S.E., Uba, S., Uzairu, A. (2020): In silico study for evaluating the binding mode and interaction of 1, 2, 4-triazole and its derivatives as potent inhibitors against Lipoate protein B (LipB). – Journal of King Saud University-Science 32(1): 475-485.
- Adzhubei, I., Jordan, D.M., Sunyaev, S.R. (2013): Predicting functional effect of human [3] missense mutations using PolyPhen-2. – Current Protocols in Human Genetics 76(1): 7-
- [4] Angamuthu, K., Piramanayagam, S. (2017): Evaluation of in silico protein secondary structure prediction methods by employing statistical techniques. - Biomedical and Biotechnology Research Journal (BBRJ) 1(1): 29-36.
- Arshad, M., Bhatti, A., John, P. (2018): Identification and in silico analysis of functional [5] SNPs of human TAGAP protein: A comprehensive study. – PloS One 13(1): 13p.
- Capriotti, E., Calabrese, R., Casadio, R. (2006): Predicting the insurgence of human [6] genetic diseases associated to single point protein mutations with support vector machines and evolutionary information. – Bioinformatics 22(22): 2729-2734.
- Carugo, O., Pongor, S. (2001): A normalized root-mean-spuare distance for comparing [7] protein three-dimensional structures. – Protein Science 10(7): 1470-1473. Choi, Y., Sims, G.E., Murphy, S., Miller, J.R., Chan, A.P. (2012): Predicting the
- [8] functional effect of amino acid substitutions and indels. – Plos One 7(10): 13p.
- [9] Colovos, C., Yeates, T.O. (1993): Verification of protein structures: patterns of nonbonded atomic interactions. – Protein Science 2(9): 1511-1519.
- Dallakyan, S., Olson, A.J. (2014): Small-molecule library screening by docking with PyRx. – In Chemical Biology: Methods and Protocols, New York, NY: Springer New York 8p.
- [11] Fareed, M.M., Ullah, S., Aziz, S., Johnsen, T.A., Shityakov, S. (2022): In-silico analysis of non-synonymous single nucleotide polymorphisms in human β-defensin type 1 gene reveals their impact on protein-ligand binding sites. - Computational Biology and Chemistry 98: 8p.
- [12] Geourion, C., Deleage, G. (1995): SOPMA: significant improvements in protein secondary structure prediction by consensus prediction from multiple alignments. -Bioinformatics 11(6): 681-684.

- [13] Gnad, F., Baucom, A., Mukhyala, K., Manning, G., Zhang, Z. (2013): Assessment of computational methods for predicting the effects of missense mutations in human cancers. BMC Genomics 14: 1-13.
- [14] Griggs, N.D., Jarpe, M.A., Pace, J.L., Russell, S.W., Johnson, H.M. (1992): The Nterminus and C-terminus of IFN-gamma are binding domains for cloned soluble IFN-gamma receptor. Journal of Immunology (Baltimore, Md.: 1950) 149(2): 517-520.
- [15] Hasnain, M.J.U., Shoaib, M., Qadri, S., Afzal, B., Anwar, T., Abbas, S.H., Sarwar, A., Talha Malik, H.M., Tariq Pervez, M. (2020): Computational analysis of functional single nucleotide polymorphisms associated with SLC26A4 gene. PLoS One 15(1): 20p.
- [16] Isaacs, A., Lindenmann, J. (1957): Virus interference. I. The interferon. Proceedings of the Royal Society of London, Series B-Biological Sciences 147(927): 258-267.
- [17] Jahandideh, S., Zhi, D. (2014): Systematic investigation of predicted effect of nonsynonymous SNPs in human prion protein gene: a molecular modeling and molecular dynamics study. Journal of Biomolecular Structure and Dynamics 32(2): 289-300.
- [18] Jumper, J., Evans, R., Pritzel, A., Green, T., Figurnov, M., Ronneberger, O., Tunyasuvunakool, K., Bates, R., Žídek, A., Potapenko, A., Bridgland, A. (2021): Highly accurate protein structure prediction with AlphaFold. Nature 596(7873): 583-589.
- [19] Kaur, S., Ali, A., Ahmad, U., Siahbalaei, Y., Pandey, A.K., Singh, B. (2019): Role of single nucleotide polymorphisms (SNPs) in common migraine. The Egyptian Journal of Neurology, Psychiatry and Neurosurgery 55: 1-7.
- [20] Khan, S.M., Faisal, A.R.M., Nila, T.A., Binti, N.N., Hosen, M.I., Shekhar, H.U. (2021): A computational in silico approach to predict high-risk coding and non-coding SNPs of human PLCG1 gene. PloS One 16(11): 22p.
- [21] Khanna, N.R., Gerriets, V. (2020): Interferon. StatPearls Publishing 6p.
- [22] Kotenko, S.V., Durbin, J.E. (2017): Contribution of type III interferons to antiviral immunity: location, location, location. – Journal of Biological Chemistry 292(18): 7295-7303.
- [23] López-Ferrando, V., Gazzo, A., De La Cruz, X., Orozco, M., Gelpí, J.L. (2017): PMut: a web-based tool for the annotation of pathological variants on proteins, 2017 update. Nucleic Acids Research 45(W1): W222-W228.
- [24] Magesh, R., George Priya Doss, C. (2014): Computational pipeline to identify and characterize functional mutations in ornithine transcarbamylase deficiency. 3 Biotech 4: 621-634.
- [25] Mahmud, Z., Malik, S.U.F., Ahmed, J., Azad, A.K. (2016): Computational Analysis of Damaging Single-Nucleotide Polymorphisms and Their Structural and Functional Impact on the Insulin Receptor. BioMed Research International 11p.
- [26] Morris, G.M., Huey, R., Olson, A.J. (2008): Using autodock for ligand-receptor docking. Current Protocols in Bioinformatics 24(1): 8-14.
- [27] Pacheco, A.G., Moraes, M.O. (2009): Genetic Polymorphisms of Infectious Diseases in Case-Control Studies. Disease Markers 27(3-4): 173-186.
- [28] Qi, Z., Nie, P., Secombes, C.J., Zou, J. (2010): Intron-containing type I and type III IFN coexist in amphibians: refuting the concept that a retroposition event gave rise to type I IFNs. The Journal of Immunology 184(9): 5038-5046.
- [29] Reynard, M. (2002): Cytokine gene polymorphisms and their clinical relevance. University of London, University College London (United Kingdom) 312p.
- [30] Sang, Y., Liu, Q., Lee, J., Ma, W., McVey, D.S., Blecha, F. (2016): Expansion of amphibian intronless interferons revises the paradigm for interferon evolution and functional diversity. Scientific Reports 6(1): 17p.
- [31] Santhoshkumar, R., Yusuf, A. (2020): In silico structural modeling and analysis of physicochemical properties of curcumin synthase (CURS1, CURS2, and CURS3) proteins of Curcuma longa. Journal of Genetic Engineering and Biotechnology 18(1): 9p.

- [32] Savan, R., Ravichandran, S., Collins, J.R., Sakai, M., Young, H.A. (2009): Structural conservation of interferon gamma among vertebrates. Cytokine & Growth Factor Reviews 20(2): 115-124.
- [33] Sim, N.L., Kumar, P., Hu, J., Henikoff, S., Schneider, G., Ng, P.C. (2012): SIFT web server: predicting effects of amino acid substitutions on proteins. Nucleic Acids Research 40(W1): W452-W457.
- [34] Trott, O., Olson, A.J. (2010): AutoDock Vina: improving the speed and accuracy of docking with a new scoring function, efficient optimization, and multithreading. Journal of Computational Chemistry 31(2): 455-461.
- [35] Xu, D., Zhang, Y. (2011): Improving the physical realism and structural accuracy of protein models by a two-step atomic-level energy minimization. Biophysical Journal 101(10): 2525-2534.
- [36] Zhang, Y., Skolnick, J. (2005): TM-align: a protein structure alignment algorithm based on the TM-score. Nucleic Acids Research 33(7): 2302-2309.
- [37] Zhang, Y., Skolnick, J. (2004): SPICKER: a clustering approach to identify near-native protein folds. Journal of Computational Chemistry 25(6): 865-871.